Available online at www.sciencedirect.com
SCIENCE DIRECT®
Biochemical Pharmacology 65 (2003) 1271–1280
Biochemical Pharmacology
www.elsevier.com/locate/biochempharm

Two-step formation of ^{1}H NMR visible mobile lipids during apoptosis of paclitaxel-treated K562 cells

Fabrizia Brisdelli[a], Egidio Iorio[b,c], Arno Knijn[b,d], Amalia Ferretti[b], Donatella Marcheggiani[a], Luisa Lenti[e], Roberto Strom[c], Franca Podo[b], Argante Bozzi[a,*]

[a]*Department of Biomedical Sciences and Technologies, University of L'Aquila, Via Vetoio, Coppito 2, 67100 L'Aquila, Italy*
[b]*Laboratory of Cell Biology, Istituto Superiore di Sanità, 00161 Rome, Italy*
[c]*Department of Cellular Biotechnology and Haematology, University "La Sapienza", 00185 Rome, Italy*
[d]*Data Management Service, Istituto Superiore di Sanità, 00161 Rome, Italy*
[e]*Department of Experimental Medicine and Pathology, University "La Sapienza", 00185 Rome, Italy*

Received 29 August 2002; accepted 14 January 2003

Abstract

Despite increasing evidence on the formation of ^{1}H NMR-detectable mobile lipid (ML) domains in cells induced to programmed cell death by continuous exposure to anticancer drugs, the time course of ML generation during the apoptotic cascade has not yet been fully elucidated. The present study shows that ML formation occurs at two different stages of apoptosis induced in human erythroleukemia K562 cells by a brief (3 hr) exposure to paclitaxel (Taxol), an antitumour drug with a stabilising effect on microtubules, or to paclitaxel *plus* tyrphostin AG957, a selective inhibitor of the $p210^{BCR\text{-}ABL}$ tyrosine kinase activity. A first wave of ML generation was in fact detected in paclitaxel-treated cells at the onset of the effector phase (8–24 hr after exposure to the drug), plateaued at 24–48 hr and was eventually followed by further ML accumulation during the degradative phase (48–72 hr). Addition of AG957 to paclitaxel shifted to the 3–8 hr interval in both the early ML production and the onset of apoptotic events, such as chromatin condensation, phosphatidylserine externalisation, cytochrome *c* release and caspase-3 activation. A significant loss of mitochondrial membrane potential was almost concomitant with the second wave of ML accumulation, associated in both cell systems with the phase of terminal cell degeneration, likely connected to non-regulated degradation of cell lipid components.

Keywords: Apoptosis; Nuclear magnetic resonance spectroscopy; K562 cells; Mobile lipids; Paclitaxel; Tyrphostin

1. Introduction

Several studies have reported the appearance of narrow mobile lipid (ML) signals in ^{1}H nuclear magnetic resonance (NMR) spectra of cells induced to apoptosis by long-term exposure to antitumour drugs or by addition of anti-Fas antibodies [1–4]. The amount of ML in Jurkat cells, evaluated from their ^{1}H NMR spectra as an increase in the intensity of the hydrocarbon chains' methylene (1.3 ppm) over the methyl (0.9 ppm) signals, has been correlated to the apoptotic cell fraction induced by exposure to anthracyclines or to dexamethasone [2,3], suggesting that ^{1}H NMR might be proposed as a new, quantitative method for a noninvasive evaluation of apoptosis in cell cultures and in tissues. This methodology can even be used [5] to differentiate apoptosis from cell necrosis. The appearance of ML can however hardly be considered, by itself, as a peculiar feature of apoptotic cells, since similar spectral patterns have also been found in activated lymphocytes and lymphoblasts [3,6,7], in tumours [8,9], in embryo-derived cells [10] and even in some adult tissues, such as colon submucosa and striated muscle [11,12]. ML signals are usually believed to arise from lipids organised in nonlamellar

* Corresponding author: Tel: +39-0862-433472; fax: +39-0862-433433.
E-mail address: bozzi@cc.univaq.it (A. Bozzi).

Abbreviations: Ac-DEVD-AMC, acetyl-Asp-Glu-Val-Asp-aminomethylcoumarin; Annexin-V-Fluos, fluoresceinated Annexin-V; AO, acridine orange; $\Delta\Psi_m$, mitochondrial membrane potential; EB, ethidium bromide; ECL, enhanced chemiluminescence; JC-1, 5,5′,6,6′-tetrachloro-1,1′,3,3′-tetraethylbenzimidazole carbocyanine iodide; ML, mobile lipids; NMR, nuclear magnetic resonance; PBS, phosphate-buffered saline; PI, propidium iodide; PtdSer, phosphatidylserine.

0006-2952/03/$ – see front matter © 2003 Elsevier Science Inc. All rights reserved.
doi:10.1016/S0006-2952(03)00080-7

domains, such as those present in cytoplasmic lipid droplets and/or in membrane embedded microdomains, characterised by a high level of isotropic mobility that allows their detection in the high resolution NMR time window [13–17].

In this work, the objective was to study in more detail the time course of ML formation in relation to the typical enzymatic and morphological changes occurring during the apoptotic cascade, specifically including the early stages along with the more generally studied advanced stages of apoptosis. To this end, NMR analyses were performed on intact human erythroleukemia K562 cells, exposed for 3 hr to the anticancer drug paclitaxel (Taxol®), which freezes microtubule dynamics, inhibits growth and cell cycle progression [18–21]. Since these erythroleukemic cells express the $p210^{BCR\text{-}ABL}$ fusion protein, that reportedly confers resistance to drug-induced apoptosis [22–24] through its high tyrosine kinase activity which is specifically inhibited by tyrphostin AG957 [25,26], some experiments were performed by exposing the cells to a combination of Taxol *plus* AG957, so as to increase their sensitivity to apoptosis inducing events. After this relatively short (pulsed) exposure to the drug(s), the cells were kept at 37° in drug-free medium for three more days, during which NMR spectra of the intact cells were recorded (at 3, 8, 24, 48 and 72 hr), whilst assessing the evolution of the apoptotic process and its extent on the basis of typical features, such as structural alterations of cell nuclei (that became hypodiploid, with a condensed chromatin and DNA laddering), Annexin-V binding to the outer side of the cell membrane, cytochrome *c* release, caspase-3 activation and irreversible mitochondrial membrane potential ($\Delta\Psi_m$) loss.

2. Materials and methods

2.1. Materials

RPMI 1640 medium, fetal calf serum and proteinase K were from Labtek-EUROBIO. Paclitaxel (Taxol®), acridine orange, ethidium bromide, propidium iodide, Nonidet P-40, RNase A, Triton X-100 and valinomycin were purchased from Sigma. Tyrphostin AG957 (4-amino-*N*-[2,5-dihydroxybenzyl]methyl benzoate) was from Calbiochem. JC-1 (5,5′,6,6′-tetrachloro-1,1′,3,3′-tetraethylbenzimidazole carbocyanine iodide) was obtained from Molecular Probes. Fluoresceinated Annexin-V (Annexin-V-Fluos), monoclonal anti-Bcl-2 and anti-actin antibodies were purchased from Roche Molecular Biochemicals. Monoclonal anti-cytochrome *c* antibody was purchased from PharMingen. Caspase-3 fluorogenic substrate Ac-DEVD-AMC (acetyl-Asp-Glu-Val-Asp-aminomethyl-coumarin) from Alexis Biochemicals. Reagents for enhanced chemiluminescence (ECL) detection were obtained from Amersham Life Science. All other chemicals were reagent grade.

2.2. Cell culture and treatment

K562 human erythroleukemic cells were maintained in exponential growth at 37° in a humidified atmosphere containing 5% CO_2, using an RPMI 1640 medium supplemented with 10% heat-inactivated fetal calf serum, 2 mM L-glutamine, 50 units/mL penicillin and 50 μg/mL streptomycin. The cells (4×10^5 cells/mL) were exposed for 3 hr to 200 nM Taxol, either alone or in combination with 50 μM tyrphostin AG957. After two washes, the cells were resuspended and incubated in drug-free medium for up to 72 hr. Cell counting and viability were determined at various times by trypan blue exclusion method.

2.3. Analysis of cell morphology

Nuclear morphology and cell viability were analysed by double AO- and EB-staining. After mixing with an equal volume of a solution that contained 100 μg/mL EB and 100 μg/mL AO, the cell suspension was examined with a fluorescence microscope [27]. Green clumped nuclei indicated chromatin condensation with intact membrane structures (early apoptosis); orange cells with clumped nuclei indicated later apoptosis. Nuclei of necrotic cells appeared uniformly stained by EB.

2.4. Cell cycle analysis

K562 cells (1.0×10^6), collected by centrifugation, were gently resuspended in 1.0 mL of a hypotonic solution containing 50 μg/mL PI in 0.1% (w/v) sodium citrate *plus* 0.1% (v/v) Triton X-100, and left overnight in the dark at 4°. The distribution of fluorescence among individual nuclei, measured with an EPICS XL-MCL cytometer equipped with a 488 nm argon laser lamp, as previously described [28], was converted, by a MULTICYCLE program, into percentage of cells in the different phases of the cell cycle.

2.5. Fluorescein isothiocyanate (FITC) Annexin-V assay

Cells (1.0×10^6) were washed in PBS and resuspended in 100 μL of a staining solution that contained 2 μL of Annexin-V-FITC (Annexin-V-Fluos) and 1 μg/mL PI in 10 mM Hepes/NaOH, pH 7.4, 140 mM NaCl, 5 mM $CaCl_2$. After incubation at room temperature for 15 min, the cells were examined in the fluorescence microscope.

2.6. DNA fragmentation assay

Control and treated samples of 1.0×10^6 cells, collected after 3, 8, 24, 48 and 72 hr after drug(s) removal, were washed with PBS and the pelleted cells were resuspended in 100 μL of lysis buffer (50 mM Tris–HCl, pH 8.0, 10 mM EDTA, 0, 25% Nonidet P-40, 1 mg/mL RNase A). After

1 hr incubation at 37° the suspension was supplemented with 1 mg/mL proteinase K and further incubated at 37° for 1 hr. Crude extracts were then diluted with a 6× "loading buffer" [29] that contained 0.25% bromophenol blue and 40% (w/v) sucrose, and DNA was fractionated by 2% (w/v) agarose gel electrophoresis.

2.7. Mitochondrial membrane potential ($\Delta\Psi_m$)

Changes in $\Delta\Psi_m$ were measured by using the lipophilic cationic probe JC-1. This molecule, able to selectively enter into mitochondria, exists in a monomeric form emitting at 527 nm upon excitation at 488 nm. However, depending on the membrane potential, JC-1 is able to form J-aggregates characterised by a large bathochromic shift in emission (590 nm). Thus, the colour of the dye changes reversibly from green to greenish orange, as the mitochondrial membrane becomes more polarised [30]. K562 cells were stained for 15 min in the dark, at 37°, with 2.5 μg/mL of JC-1 and, after two washes with ice-cold PBS, they were immediately analysed in the EPICS XL-MCL flow cytometer. A positive control sample, obtained by adding 100 nM valinomycin (a well known K^+-ionophore), was included in each experiment. Loss of $\Delta\Psi_m$ in K562 cells was evaluated by measuring the variations of fluorescence emission at 527 nm.

2.8. Assay of caspase-3-like protease activity

Frozen cell pellets were dissolved by leaving them for 30 min on ice in a lysis buffer containing 50 mM Tris–HCl (pH 7.4), 10 mM EGTA, 1 mM EDTA and 1% (v/v) Triton X-100. The protein concentration of the cleared lysates was determined according to Bradford's method [31] and 60 μg of proteins were incubated at 37° for 30 min in a reaction mixture containing 20 μM Ac-DEVD-AMC. Fluorescence was monitored, on a Perkin-Elmer LS-50B spectrofluorometer, setting excitation at 380 nm and emission at 460 nm.

2.9. Western blotting

Proteins were extracted from cells by suspending them for 30 min at 4° in a buffer that contained 10 mM Hepes, pH 7.2, 0.142 M KCl, 5 mM $MgCl_2$, 1 mM EDTA, 0.2% Nonidet P-40 and an appropriate cocktail of protease inhibitors. Cell lysates were centrifuged at 4° in an Eppendorf microfuge at 15,000 *g* and the clear supernatants subjected to 12.5% SDS–PAGE followed by electroblotting to polyvinylidene difluoride membranes. The membranes were then probed with a monoclonal anti-Bcl-2 antibody (1:100 dilution) or with a monoclonal anti-actin antibody (1:7000 dilution), followed by an anti-mouse peroxidase-conjugated secondary IgG antibody. Immune complexes were detected by ECL and exposed to a Kodak X-OMAT film.

2.10. Cytochrome c release

Cells were washed twice with PBS and pellets were resuspended in permeabilisation buffer (250 mM sucrose, 20 mM HEPES, 10 mM KCl, 1.5 mM Na-EGTA, 1.5 mM Na-EDTA, 1 mM $MgCl_2$, 1 mM dithiothretol, 50 μg/mL digitonin, pH 7.4, containing a suitable cocktail of protease inhibitors) for 10 min at 4°. Permeabilised cells were centrifuged (800 *g*, 15 min) at 4°. The clear supernatants were further centrifuged (18,000 *g*, 30 min) at the same temperature. After determination of protein concentration [31], a 25 μg sample was loaded and separated on a 15% SDS–PAGE and probed with anti-cytochrome *c* antibody (7H8.2C12) as described above.

2.11. NMR spectra and data analysis

One-dimensional ^1H NMR experiments on intact K562 cell preparations (30–40 × 10^6 in 0.5 mL PBS/D_2O) were carried out at 400 MHz on a Bruker AVANCE 400 WB spectrometer, at 25°, using 60° pulses preceded by 1.0 s presaturation for water signal suppression (spectral width 10 ppm), the total measurement time being 17 min for 320 scans. Signal processing and quantitative data analysis on proton spectra of $(CH_2)_n$ arising from fatty acid chains of ML, lactate and other water-soluble metabolites were performed using the Bruker WIN-NMR software package. Signal processing consisted of zero-filling the free induction decays from 32 K data points to 64 K before discrete Fourier transformation. After having fitted the baseline in the frequency domain with a cubic splines model through appropriate points, the peaks of interest (and nearby interfering peaks) were modelled by deconvolution, assuming Lorentzian lineshapes. Since the intensity of the contribution of β and δ methylene protons of lysine to the signal at 1.7 ppm remained apparently invariant during cell sample manipulation, the deconvoluted area of the lysine signals was preferred, as a reference, to the more generally used CH_3 peak at 0.9 ppm. In this study, however, this change of reference did not influence the global courses of the signals under investigation, indicating that also the CH_3 peak intensity remained largely stable.

2.12. Statistical analysis

Differences were considered statistically significant for *P*-values, determined by Student's *t*-test, lower than 0.05.

3. Results

3.1. Effects of pulsed Taxol treatment

As mentioned in Section 1, we have examined the time course of the apoptotic response of K562 cells exposed

either to Taxol alone or to Taxol *plus* tyrphostin AG957. After 3 hr-exposure to 200 nM Taxol, K562 cells showed—as already reported by other authors [32]—no apparent immediate cell damage. During their subsequent incubation in drug-free medium at 37°, a sizeable fraction of these Taxol-treated cells (K562-TX) underwent a transient cell cycle arrest in the G_2M phase and progressively exhibited—though remaining for over 72 hr impermeable to trypan blue—morphological and enzymatic features of programmed cell death, such as alterations of nuclear staining properties, phosphatidylserine (PtdSer) externalisation, cytochrome *c* release, caspase-3 activation, $\Delta\Psi_m$ loss, and DNA laddering. These apoptotic parameters were quantitatively monitored, in parallel with NMR measurements of ML production, at different times of cell incubation after exposure to the drug. ^{1}H NMR analyses, illustrated in Fig. 1 by some representative spectra and quantified in detail in Fig. 2, showed between 8 and the 24 hr a significant, progressive increase in the intensity of ML $(CH_2)_n$ signals from K562-TX cells. After an intermediate plateau (24–48 hr), a second sharp increase in the intensity of these signals occurred at 48–72 hr (Figs. 1 and 2). The amount of ML formed at 8–24 hr represented about one-third of the total ML produced by K562-TX cells during the overall 72 hr of post-Taxol incubation.

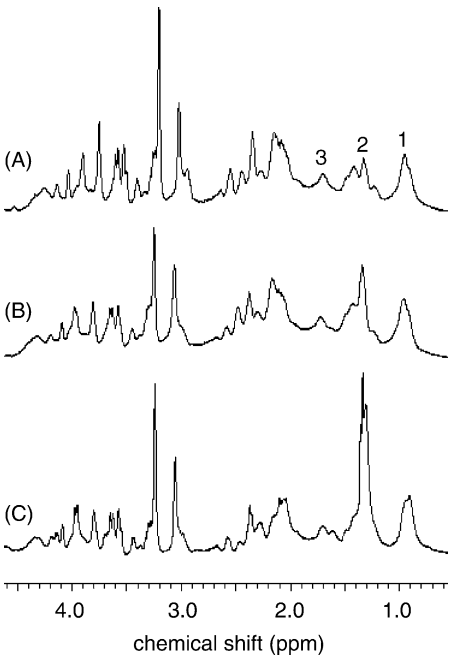

Fig. 1. ^{1}H NMR spectra of intact K562 cell preparations. Cells underwent treatment for 3 hr and were subsequently observed after different time intervals of incubation in drug-free medium. (A) Control cells, observed after 3 hr; (B) cells treated with 200 nM Taxol *plus* 50 μM tyrphostin AG957 (K562-TX/AG), observed after 8 hr; and (C) cells treated with 200 nM Taxol (K562-TX), observed after 72 hr. Peak assignments: (1) CH_3 from amino acids or small proteins and MLs, with a possible contribution of cholesterol (C-18, -19, -21, -25, -26); (2) $(CH_2)_n$ from MLs, as well as from lactate CH_3, whose resonance can be isolated by appropriate deconvolution; (3) CH_2 (β, δ) from lysine, whose partial overlap with the $COCH_2\underline{CH}$ protons can be resolved by deconvolution.

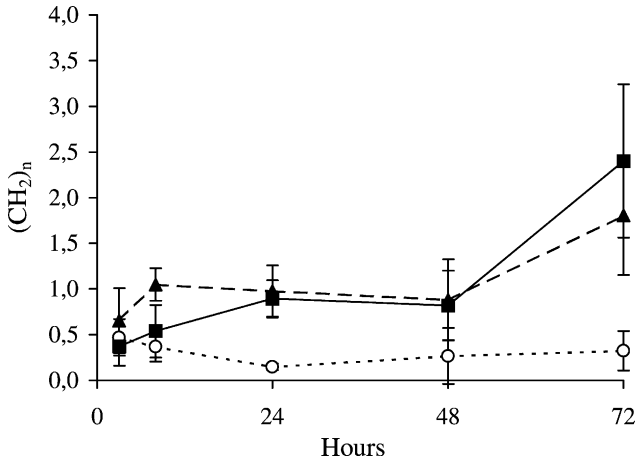

Fig. 2. Time course of the relative peak area of ^{1}H NMR visible ML $(CH_2)_n$ signals in K562 cells treated with either 200 nM Taxol (K562-TX, —■—) or Taxol *plus* 50 μM tyrphostin AG957 (K562-TX/AG, –▲-) or as untreated control (····○····) for 3 hr. NMR spectra were recorded after 3, 8, 24, 48 and 72 hr incubation in drug-free medium. The $(CH_2)_n$ peak areas were quantified with respect the CH_2 (β, δ) peak from lysine. Values are expressed in arbitrary units and the results represent the mean ± SD values obtained from at least three independent experiments. Statistically significant differences were present at 8 hr in K562-TX/AG vs. control and vs. K562-TX cells ($0.02 < P < 0.05$); at 24 and 72 hr in both K562-TX/AG and K562-TX vs. control ($P < 0.005$). For K562-TX cells, the bimodal pattern was confirmed by statistical analysis: the $(CH_2)_n$ peak area changed significantly ($P < 0.025$) during the 8–24 and 48–72 hr intervals, but remained practically invariant ($P > 0.2$) from 24 to 48 hr.

The first wave of ML formation occurred in parallel with the detection in these cells of typical apoptotic features, such as chromatin condensation (Fig. 3A) and PtdSer externalisation (Fig. 3B). These parameters started to increase between 8 and 24 hr after the pulsed exposure to Taxol, and progressively increased thereafter. Moreover, a substantial hypodiploid (''sub-Go'') subpopulation accumulated in the same time interval (Fig. 4A), following a sharp but transient peak of the cell fraction in the G_2M phase of the cycle (Fig. 4B). As compared to this series of relatively early markers, cytochrome *c* release started to be detected around 24 hr (Fig. 5A), when first signs of caspase-3 activation and $\Delta\Psi_m$ dissipation were also observed (Fig. 5B and C). As shown in Fig. 6, a distinct DNA laddering was detected at a much later stage (72 hr).

In no case was it possible to detect, in K562 cells, any quantitative alteration in the levels of Bcl-2, Bcl-X_L, Bad and Bax proteins (data not shown). A qualitative immunoblot analysis showed, however, 8 hr after the end of the treatment with Taxol, the presence of a second, more slowly migrating Bcl-2 band (Fig. 7), that can probably be attributed—in line with the well known post-translational modification of this protein in cells treated with tubulin-targeted agents [33]—to a transient phosphorylation, associated with the mitotic arrest in G_2M phase.

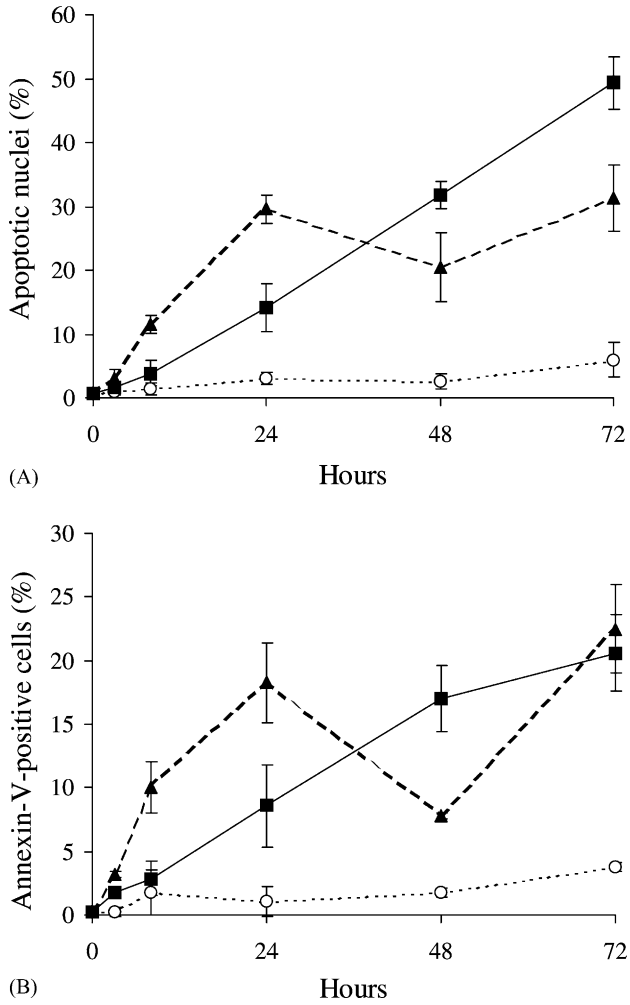

Fig. 3. Time course of nuclear condensation (A) and of PtdSer externalisation (B) in K562 cells treated for 3 hr with either 200 nM Taxol (K562-TX, —■—) or Taxol *plus* 50 μM tyrphostin AG957 (K562-TX/AG, –▲–), or in untreated controls (····○····). These apoptotic cell death parameters were evaluated either immediately or after 3, 8, 24, 48 and 72 hr incubation in drug-free medium. The percentage of condensed or fragmented nuclei was estimated on AO- and EB-double-stained cells, examined in the fluorescence microscope. PtdSer externalisation was estimated by an Annexin-V-FITC assay on cells examined in the fluorescent microscope; data are expressed as percent of Annexin-V-positive cells. Slides were examined in a random order and at least 400 cells were counted for each determination. The results represent the mean ± SD values obtained from three independent experiments. Statistically significant differences were present both in Fig. 3A and B at 8 hr in K562-TX/AG vs. control ($P < 0.02$); at 24 hr in K562-TX/AG vs. control ($P < 0.001$) and in K562-TX vs. control ($P < 0.01$).

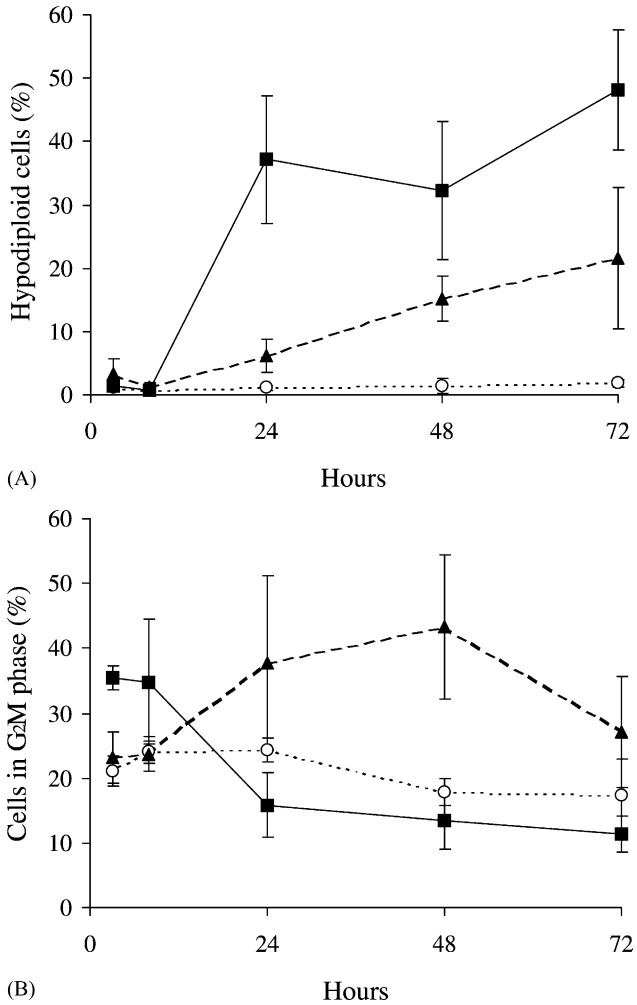

Fig. 4. Cytofluorimetric analysis of cell cycle in PI-stained K562 cells after treatment with either 200 nM Taxol (K562-TX, —■—) or Taxol *plus* 50 μM tyrphostin AG957 (K562-TX/AG, –▲–) or untreated control (····○····) for 3 hr. Measurements were performed after 3, 8, 24, 48 and 72 hr incubation in drug-free medium. Data represent mean ± SD values of the percentages of cells with hypodiploid nuclei (A) or in the G_2M phase (B), measured in at least three independent experiments. Statistically significant differences were observed in the percent of hypodiploid cells at 24 hr in K562−TX vs. control as well as vs. K562-TX/AG ($P < 0.002$ in both cases); at 72 hr in K562-TX vs. control ($P < 0.004$) and vs. K562-TX/AG ($P < 0.02$). Also the percent of cells in G_2M phase were significantly different ($P < 0.04$ in both cases), at 3 hr, in K562-TX vs. either control or K562-TX/AG, as well as, at 24–48 hr, in K562-TX vs. control ($P < 0.007$) or vs. K562−TX/AG ($0.01 < P < 0.05$).

3.2. Modifications by combined pulsed treatment with Taxol and tyrphostin AG957

When tyrphostin AG957 (which by itself did not affect any of these apoptotic markers—data not shown) was added to Taxol during the pulsed 3 hr preincubation, the first wave of ML production in the cells (K562-TX/AG) was shifted from 8–24 to 3–8 hr of incubation in drug-free medium (as shown by a representative spectrum in Fig. 1 and the quantitative data in Fig. 2, dashed line). After a plateau between 24 and 48 hr, a second wave of ML production occurred at 48–72 hr—similar to that observed in cells treated with Taxol alone.

The earlier formation of ML in K562-TX/AG cells was concomitant with an earlier onset (at 3–8 hr) and a more rapid increase in time of apoptotic markers, such as chromatin condensation and PtdSer externalisation (Figs. 3A and B). The anticipated appearance of these apoptotic markers in cells treated with Taxol *plus* AG957 was followed by a temporary decline up to 48 hr, and then

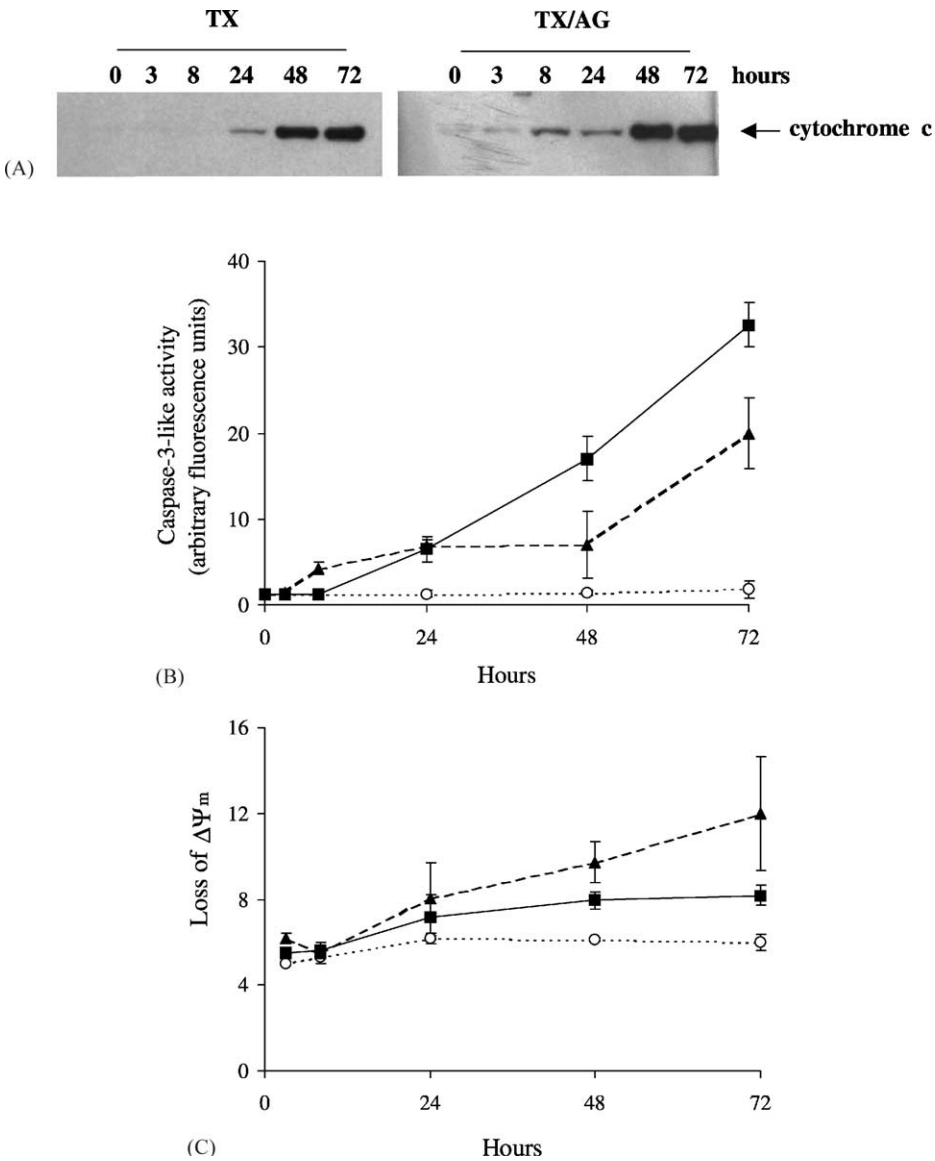

Fig. 5. Time course of (A) cytochrome *c* release, (B) caspase-3-like activity, and (C) loss of mitochondrial membrane potential ($\Delta\Psi_m$) in K562 cells in K562 cells treated for 3 hr with either 200 nM Taxol (K562-TX, —■—) or Taxol *plus* 50 μM tyrphostin AG957 (K562-TX/AG, –▲–) or untreated control (····○····). These apoptotic parameters were measured after 3, 8, 24, 48 and 72 hr of incubation in drug-free medium. Cytochrome *c* was detected in the supernatant of permeabilised cells by protein separation on 15% SDS–PAGE and detection with anti-cytochrome *c* antibody. No cytochrome *c* band could be detected in control cells at any time of incubation (data not shown). The caspase-3-like activity was measured in the cytosol of cells by using DEVD-aminomethylcoumarin as a substrate; the results represent the mean ± SD values of at least three independent experiments. $\Delta\Psi_m$ was estimated by cytofluorimetric analysis of JC-1 stained cells and was expressed in arbitrary units of fluorescence intensity. The data represent mean green fluorescence intensity (527 nm) ±SD values. No significant differences were detected in the loss of $\Delta\Psi_m$ in K562-TX vs. either control or K562-TX/AG at 24 hr; statistically significant differences were instead found at 48 hr in K562-TX vs. control ($P < 0.01$), in K562-TX/AG vs. control ($P < 0.02$) and in K562−TX vs. K562−TX/AG ($P < 0.05$); at 72 hr in K562-TX/AG vs. control ($P < 0.02$) and vs. K562-TX ($P < 0.004$).

by a final ''late'' increase, that generated an overall biphasic behaviour. The first detection of cytochrome *c* release and caspase-3 activation were also shifted from 24 to 3–8 hr (Figs. 5A and B), while $\Delta\Psi_m$ started to undergo a slowly progressing loss (Fig. 5C). On the other hand, as shown in Fig. 4B, K562-TX cells underwent, 3–8 hr after drug treatment, a clear but transient G_2M block, while in K562-TX/AG cells, in spite of the accelerated induction of most apoptotic markers, a substantial and more prolonged alteration in the G_2M population took place in K562-TX/AG cells only at 24–48 hr. Correspondingly, also the more slowly migrating Bcl-2 band was only detected at a later stage, that is, 24 hr after the end of exposure to the drug combination (Fig. 7). Furthermore, the final extent of Taxol-dependent cell death—estimated on the basis of hypodiploidy in the 48–72 hr time interval (Fig. 4A)—was also lower in K562-TX-AG than in K562-TX cells and no DNA laddering could be detected at least up to 72 hr (Fig. 6).

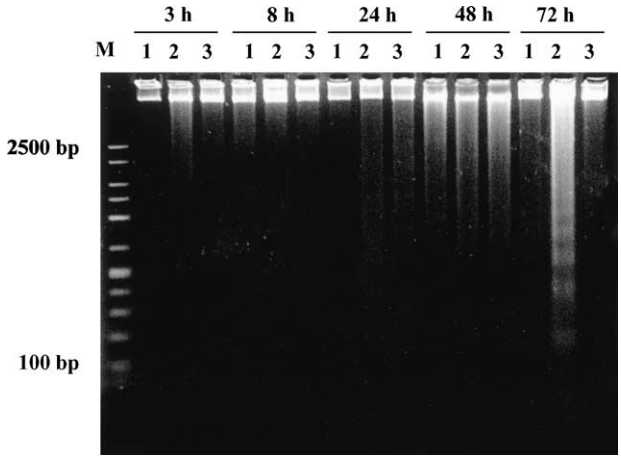

Fig. 6. Agarose gel electrophoresis of DNA isolated from (1) untreated K562; (2) K562-TX cells (treated with 200 nM Taxol) and (3) K562-TX/AG cells (treated with 200 nM Taxol *plus* 50 μM tyrphostin AG957). Cell preparations were analysed after 3, 8, 24, 48, and 72 hr of incubation in drug-free medium. (M) DNA molecular weight markers.

4. Discussion

Cellular apoptosis, from the point of view of ML generation, might in principle be just one of a number of stressful conditions which induce cells to generate, from microdomains of the endoplasmic reticulum that contain enzymes involved in lipid biosynthesis [34], lipid bodies that are not necessarily identical under all conditions. Recent ^{1}H NMR studies have indeed shown that detection of ML signals was associated to the intracellular accumulation of distinct osmiophilic lipid bodies in rat glioma cells induced to apoptosis by gene therapy *in vivo* [35], as well as in T-lymphoblastoid cells exposed *in vitro* for 72 hr to an apoptotic agent [3]. In some cell systems, such as NIH-3T3 fibroblasts and T-lymphoblastoid cells ''activated'' by treatment with phorbol myristate *plus* ionomycin, not only cytoplasmic lipid bodies (of about 1 μm diameter) but also smaller (60–100 nm diameter) amorphous lipid aggregates were detected in the context of their plasma membranes, whose likely contribution to the ML signals is still to be clarified [3,13]. As suggested by Kroemer *et al.* [36], the apoptotic process can be schematically divided in at least three functionally distinct phases, initiation, effector and degradation. By adapting a similar description to our system, our data would indicate that, following the initiation phase during the pulsed exposure to Taxol, the effector phase became detectable between 8 and 24 hr of further incubation of K562−TX cells in drug-free medium. During this time interval, a coordinated series of regulated metabolic reactions led to the onset of typical apoptotic events, such as chromatin condensation, PtdSer externalisation, release from mitochondria of an apoptogenic factor (cytochrome *c*), caspase-3 activation and hypodiploidy. Our results on the time course of the cell cycle block in G_2M in K562-TX cells are in good agreement with the well known reversibility of the effects of Taxol on microtubule dynamics [37]. Whether the G_2M block is indeed involved in the pathway to Taxol-induced apoptosis is still under debate [38,39]. According to Wang *et al.* [21], ''paclitaxel-induced apoptosis can occur either directly after a mitotic arrest or following an aberrant mitotic exit into a G_1-like 'multinucleate state' ''. In this context, it is interesting to note that in K562-TX/AG cells, as compared to K562-TX, a delayed (at 24–48 hr) and more prolonged block in G_2M was actually associated with a lower extent of late apoptosis. When the initiation phase was triggered by Taxol in the presence of tyrphostin AG957, the onset of the effector phase was anticipated to be 3–8 hr. Cytochrome *c* release also had an earlier onset at 3–8 hr. These phenomena were most likely a consequence of the specific inhibition by AG957 of the $p210^{BCR\text{-}ABL}$ tyrosine kinase activity, a mechanism which would in fact be expected to facilitate apoptosis.

However, not all apoptotic steps were accelerated by AG957 throughout the cell death programme. In fact, the cell population in G_2M increased much more slowly and was maintained for a longer time in K562-TX/AG than in K562-TX cells. Both the delay in the G_2M block and the later detection of a second Bcl-2 electrophoretic component would actually be in line with the existence of a tight connection of Bcl-2 phosphorylation with the G_2M phase

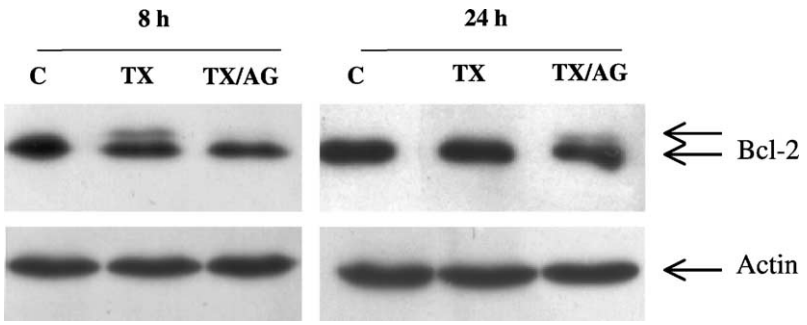

Fig. 7. Western blot analysis of Bcl-2 protein, detected by monoclonal anti-Bcl-2 antibody, in lysates (60 μg proteins/lane) of (C) untreated, (TX) Taxol- and (TX/AG) Taxol + tyrphostin AG957-treated K562 cells after 8 and 24 hr of incubation in drug-free medium. A monoclonal anti-actin antibody was used as a control.

of the cell cycle [40] rather than with a reduced inhibition of the apoptotic process. Moreover, some markers detected at both early and late stages (e.g. chromatin condensation and PtdSer externalisation) instead of continuing to increase in time, as in K562-TX cells, exhibited a biphasic behaviour in K562-TX/AG cells (i.e. a first increase within the first 24 hr was followed by a decline at 24–48 hr and then by a further increase at the latest stage of the apoptotic process). Lastly, cell exposure to Taxol *plus* AG957 resulted in a significant delay and/or inhibition of some of the latest apoptotic steps (such as DNA laddering). The delay or slowing-down in the detection of intermediate and late markers of apoptosis in K562-TX/AG cells can be tentatively explained on the basis of the well known competition of tyrphostins with ATP binding sites of several proteins, with the consequent transient paralysis of ATP-dependent steps of the apoptotic enzymic cascade—including presumably those involved in the ladder-type DNA fragmentation [26].

As a first set of conclusions, the results obtained in this study indicate that (a) in spite of the differences in the time course (and underlying mechanisms) of the apoptotic events respectively monitored in K562-TX and in K562-TX/AG cells, a rather clear-cut distinction was allowed between some early and late markers of the apoptotic cascade; (b) during this process, a first production of ML occurred, in both cell systems, more or less concomitant to chromatin condensation, PtdSer externalisation and cytochrome *c* release, even before major caspase-3 activation and $\Delta\Psi_m$ loss; (c) the second wave of ML generation occurred during the degradative phase of programmed cell death (48–72 hr) after an intermediate plateau (24–48 hr), concomitant with the loss of mitochondrial membrane potential; and (d) only in K562-TX cells a marked DNA ladder was detectable at 72 hr upon drug exposure.

Analysis of the two-step pattern of ML formation, in parallel with that of concomitant apoptotic markers, opens new possibilities of monitoring the time course of the apoptotic cascade in an intact cell system and also allows additional hypotheses on the molecular mechanisms possibly responsible for the generation of ML during the apoptotic cascade.

There are still unanswered questions regarding biogenesis, nature and time course of generation of NMR-detectable MLs during the apoptotic process. At variance from other markers, ML formation can be monitored in intact cells undergoing apoptosis, but their relationship to apoptosis itself and to the known pathways of propagation of this process is as yet to be clarified.

An earlier ^{1}H NMR study [2] had for instance suggested, on the basis of a correlation between ML signals and exposure of PtdSer on the outer membrane leaflet, that generation of ML domains be associated with the loss of membrane phospholipid asymmetry in the course of the apoptotic process, similar to that observed. This hypothesis might hold for the ML signals generated at early times (8 hr) in K562-TX/AG cells (Fig. 2) which are also characterised by a significantly higher exposure of PtdSer, as compared to the control ($P < 0.02$), (Fig. 3B). However, an even higher PtdSer externalisation was observed in K562-TX/AG cells at 24 hr after drug treatment, which was not associated with further ML signal enhancement with respect to the same cells at 8 hr, nor vs. K562-TX cells at 24 hr. These data seem to indicate that PtdSer externalisation may not be sufficient, by itself, to provide a full explanation to the first wave of ML production in our cell systems.

A more recent study [5] suggested that the higher ML visibility could be due to an increase in ceramide during apoptosis. Generation and accumulation of ceramides, either through the sequential activation of a phosphatidylcholine-specific phospholipase C and of an acidic sphingomyelinase [41] or through a block in glucosylceramide formation [42], has indeed been linked to enhanced apoptotic responses [43,44]. Ceramides and related metabolites, though probably only if present in relatively large amounts, can also contribute to the formation of NMR visible ML structures, such as cytoplasmic lipid droplets [45] and/or mobile-lipid membrane domains [46]. Moreover, by coalescing into these structures, ceramide metabolites would be partially diverted from activating the mitochondrial pathway to apoptosis, a mechanism that might also explain the delay in mitochondrial membrane potential dissipation, observed in our cell systems.

It has been proposed that mitochondrial function impairment is associated with the formation of NMR visible lipids in cells treated with drugs interfering with the mitochondrial structure and function [47]. However, in our system the first signs of cytochrome *c* release could be detected only somewhat later than the first wave of ML production, and before detection of any substantial $\Delta\Psi_m$ loss. On the other hand, the fact that cytochrome *c* release was not simultaneous with, but rather started to occur before mitochondrial membrane depolarisation seems to be consistent with a series of recent reports on different apoptotic cell systems [48,49]. It should therefore be concluded that, under our conditions, NMR visible lipids formed during the effector phase are unlikely due to mitochondrial impairment.

The mitochondrial potential loss detected at the latest stage of the apoptotic cascade may, instead, represent one of the mechanisms responsible for the second wave of ML formation observed in both K562-TX and K562-TX/AG cells, together with the irreversible activation of degradative enzymes, such as caspases and phospholipases during terminal cell degeneration [50,51].

In conclusion, the novel observation that NMR visible ML are produced in K562 cells by two-step process, respectively related to the effector and to the degradative phase of apoptosis may offer new ways of monitoring the evolution of the cell death programme in intact cancer cells exposed to some antitumour drugs.

Acknowledgments

The present work is dedicated to the memory of Professor Franco Tatò and of his relentless enthusiasm in biological research. This investigation was supported by grants from MURST and from CNR Target Project on Biotechnology (contract no. 01045.49). We thank Massimo Giannini for excellent technical assistance and maintenance of NMR equipment.

References

[1] Blankenberg FG, Storrs RW, Naumovski L, Goralski T, Spielman D. Detection of apoptotic cell death by proton magnetic resonance spectroscopy. Blood 1996;87:1951–6.

[2] Blankenberg FG, Katsikis PD, Storrs RW, Beaulieu C, Spielman D, Chen JY, Naumovski L, Tait JF. Quantitative analysis of apoptotic cell death using proton nuclear magnetic resonance spectroscopy. Blood 1997;89:3778–86.

[3] Di Vito M, Lenti L, Knijn A, Iorio E, D'Agostino F, Molinari A, Calcabrini A, Stringaro A, Meschini S, Arancia G, Bozzi A, Strom R, Podo F. ^{1}H NMR-visible mobile lipid domains correlate with cytoplasmic lipid bodies in apoptotic T-lymphoblastoid cells. Biochim Biophys Acta—Mol Cell Biol Lipids 2001;1530:47–66.

[4] Al-Saffar NMS, Titley JC, Robertson D, Clarke PA, Jackson LE, Leach MO, Ronen SM. Apoptosis is associated with triacylglycerol accumulation in Jurkat T-cells. Br J Cancer 2002;86:963–70.

[5] Bezabeh T, Mowat MRA, Jarolim L, Greenberg AH, Smith ICP. Detection of drug-induced apoptosis and necrosis in human cervical carcinoma cells using ^{1}H NMR spectroscopy. Cell Death Differ 2001;8:219–24.

[6] Veale MF, Dingley AJ, King GF, King NJC. ^{1}H NMR visible neutral lipids in activated T lymphocytes: relationship to phosphatidylcholine cycle. Biochim Biophys Acta—Lipids and Lipid Metabol 1996;1303: 215–21.

[7] Veale MF, Roberts NJ, King GF, King NJC. The generation of ^{1}H NMR-detectable mobile lipid in stimulated lymphocytes: relationship to cellular activation, the cell cycle, and phosphatidylcholine-specific phospholipase C. Biochem Biophys Res Commun 1997;239:868–74.

[8] Mountford CE, Lena CL, Mackinnon WB, Russell P. The use of proton MR in cancer pathology. In: Webbs GA, editor. Annual reports on NMR spectroscopy. New York: Academic Press; 1993. p.173–215

[9] Mountford CE, Mackinnon WB, Russell P, Rutter A, Delikatny EJ. Human cancers detected by proton MRS and chemical shift imaging ex vivo. Anticancer Res 1996;16:1521–32.

[10] May GL, Wright LC, Holmes KT, Williams PG, Smith IC, Wright PE, Fox RM, Mountford CE. Assignment of methylene proton resonances in NMR spectra of embryonic and transformed cells to plasma membrane triglyceride. J Biol Chem 1996;261:3048–53.

[11] Bezabeh T, Smith ICP, Krupnik E, Somorjai RL, Kitchen DG, Bernstein CN, Pettigrew NM, Bird RP, Lewin KJ, Briere KM. Diagnostic potential for cancer via ^{1}H magnetic resonance spectroscopy of colon tissue. Anticancer Res 1996;16:1553–8.

[12] Howald H, Boesch C, Kreis R, Matter S, Billeter R, Essen-Gustavsson B, Hoppeler H. Content of intramyocellular lipids derived by electron microscopy, biochemical assays, and ^{1}H-NMR spectroscopy. J Appl Physiol 2002;92:2264–72.

[13] Ferretti A, Knijn A, Iorio E, Pulciani S, Giambenedetti M, Molinari A, Meschini S, Stringaro A, Calcabrini A, Freitas I, Strom R, Arancia G, Podo F. Biophysical and structural characterization of ^{1}H NMR-detectable mobile lipid domains in NIH-3T3 fibroblasts. Biochim Biophys Acta—Mol Cell Biol Lipids 1999;1438:329–48.

[14] Mountford CE, Wright LC. Organization of lipids in the plasma membranes of malignant and stimulated cells: a new model. Trends Biochem Sci 1998;13:172–7.

[15] Remy C, Fouilhé N, Barba I, Sam-Lai E, Lahrech H, Cucurella MG, Izquierdo M, Moreno A, Ziegler A, Massarelli R, Décors M, Arùs C. Evidence that mobile lipids detected in rat brain glioma by ^{1}H nuclear magnetic resonance correspond to lipid droplets. Cancer Res 1997; 57:407–14.

[16] Barba I, Cabañas ME, Arús C. The relationship between nuclear magnetic resonance—visible lipids, lipid droplets and cell proliferation in cultured C6 cells. Cancer Res 1999;59:1861–8.

[17] Hakumäki JM, Kauppinen RA. ^{1}H NMR visible lipids in the life and death of cells. Trends Biochem Sci 2000;25:9–14.

[18] Strobel T, Kraeft SK, Chen LB, Cannistra A. Bax expression is associated with enhanced intracellular accumulation of paclitaxel: a novel role for bax during chemotherapy-induced cell death. Cancer Res 1998;58:4776–81.

[19] Kavallaris M, Burkhart CA, Horwitz SB. Antisense oligonucleotides to class III beta-tubulin sensitize drug-resistant cells to Taxol. Br J Cancer 1999;80:1020–5.

[20] Glass-Marmor L, Beitner R. Taxol (Paclitaxel) induces a detachment of phosphofructokinase from cytoskeleton of melanoma cells and decreases the levels of glucose 1,6-bisphosphate, fructose 1,6-bisphosphate and ATP. Eur J Pharmacol 1999;370:195–9.

[21] Wang TH, Wang HS, Soong YK. Paclitaxel-induced cell death. Cancer 2000;88:2619–28.

[22] Bedi A, Barber JP, Bedi GC, el-Deiry WS, Sidranski D, Vala MS, Akhtar AJ, Hilton J, Jones RJ. BCR-ABL-mediated inhibition of apoptosis with delay of G2/M transition after DNA damage: a mechanism of resistance to multiple anticancer agents. Blood 1995; 86:1148–58.

[23] Cortez D, Kadlec L, Pendergast AM. Structural and signaling requirements for BCR-ABL-mediated transformation and inhibition of apoptosis. Mol Cell Biol 1995;15:5531–41.

[24] Riordan FA, Bravery CA, Mengubas K, Ray N, Borthwick NJ, Akbar AN, Hart SM, Hoffbrand AV, Metha AB, Wickremasinghe RG. Herbimycin A accelerates the induction of apoptosis following etoposide treatment or gamma-irradiation of BCR/ABL-positive leukemia cells. Oncogene 1998;16:1533–42.

[25] Beran M, Cao X, Estrov Z, Jeha S, Jin G, O'Brien S, Talpaz M, Arlinghaus RB, Lydon NB, Kantarjian H. Selective inhibition of cell proliferation and BCR-ABL phosphorylation in acute lymphoblastic leukemia cells expressing Mr 190,000 BCR-ABL protein by a tyrosine kinase inhibitor (CGP-57148). Clin Cancer Res 1998;4:1661–72.

[26] Sun X, Layton JE, Elefanty A, Lieschke GJ. Comparison of effects of the tyrosine kinase inhibitors AG957, AG490, and STI571 on BCR-ABL-expressing cells, demonstrating synergy between AG490 and ST1571. Blood 2001;97:2008–15.

[27] McGahon AJ, Martin SJ, Bissonnette RP, Mahboubi A, Shi Y, Mogil RJ, Nishioka WK, Green DR. The end of the (cell) line: methods for the study of apoptosis in vitro. Methods Cell Biol 1995;46:153–85.

[28] Nicoletti I, Migliorati G, Pagliacci F, Grignani C, Riccardi C. A rapid and simple method for measuring thymocyte apoptosis by propidium iodide staining and flow cytometry. J Immunol Methods 1991;39:271–9.

[29] Sambrook J, Fritsch EF, Maniatis T. Molecular cloning: a laboratory manual. 2nd ed. NewYork: Cold Spring Harbor; 1989.

[30] Cossarizza A, Baccarani-Contri M, Kalashnikova G, Franceschi C. A new method for the cytofluorimetric analysis of mitochondrial membrane potential using the J-aggregate forming lipophilic cation 5,5′,6,6′-tetrachloro-1,1′,3,3′-tetraethylbenzimidazolo-carbocyanine iodide (JC-1). Biochem Biophys Res Commun 1993;97:40–5.

[31] Bradford MM. A rapid and sensitive method for the quantitation of microgram quantities of protein utilizing the principle of protein–dye binding. Anal Biochem 1976;72:248–54.

[32] Gangemi RM, Santamaria B, Bargellesi A, Cosulich E, Fabbi M. Late apoptotic effects of taxanes on K562 erythroleukemia cells: apoptosis

is delayed upstream of caspase-3 activation. Int J Cancer 2000; 85:527–33.

[33] Chadebech P, Brichese L, Baldin V, Vidal S, Valette A. Phosphorylation and proteasome-dependent degradation of Bcl-2 in mitotic-arrested cells after microtubule damage. Biochem Biophys Res Commun 1999;262:823–7.

[34] Murphy DJ, Vance J. Mechanisms of lipid-body formation. Trends Biochem Sci 1999;24:109–15.

[35] Hakumäki JM, Poptani H, Sandmair AM, Herttuala SY, Kauppinen RA. ^{1}H MRS detects polyunsaturated fatty acid accumulation during gene therapy of glioma: implications for the in vivo detection of apoptosis. Nat Med 1999;5:1323–7.

[36] Kroemer G, Zamzami N, Susin SA. Mitochondrial control of apoptosis. Immunol Today 1997;18:44–51.

[37] Lieu CH, Chang YN, Lai YK. Dual cytotoxic mechanism of submicromolar Taxol on human leukemia HL-60 cells. Biochem Pharmacol 1997;53:1587–96.

[38] Fan W. Possible mechanisms of paclitaxel-induced apoptosis. Biochem Pharmacol 1999;57:1215–21.

[39] Sena G, Onado C, Cappella P, Montalenti F, Ubezio P. Measuring the complexity of cell-cycle arrest and killing of drugs: kinetics of phase-specific effects induced by Taxol. Cytometry 1999;37:113–24.

[40] Ling YH, Tornos C, Perez-Soler R. Phosphorylation of Bcl-2 is a marker of M-phase events and not a determinant of apoptosis. J Biol Chem 1998;273:18984–91.

[41] Cifone MG, Roncaioli P, De Maria R, Camarda G, Santoni A, Ruberti G, Testi R. Multiple pathways originate at the Fas/APO-1 (CD95) receptor: sequential involvement of phosphatidylcholine-specific phospholipase C and acidic sphingomyelinase in the propagation of the apoptotic signal. EMBO J 1995;14:5859–68.

[42] Senchenkov A, Litvak DA, Cabot MC. Targeting ceramide metabolism—a strategy for overcoming drug resistance. J Natl Cancer Inst 2001;93:347–57.

[43] Scaffidi C, Schmitz I, Zha J, Korsmeyer SJ, Krammer PH, Peter ME. Differential modulation of apoptosis sensitivity in CD95 type I and type II cells. J Biol Chem 1999;274:22532–8.

[44] De Maria R, Lenti L, Malisan F, d'Agostino F, Tomassini B, Zeuner A, Rippo MR, Testi R. Requirement for GD3 ganglioside in CD95- and ceramide-induced apoptosis. Science 1997;277: 1652–5.

[45] Morjani H, Aouali N, Belhoussine R, Veldman RJ, Levade T, Manfait M. Elevation of glucosylceramide in multidrug-resistant cancer cells and accumulation in cytoplasmic droplets. Int J Cancer 2001;94: 157–65.

[46] Ferretti A, Knijn A, Raggi C, Sargiacomo M. High-resolution proton NMR measures mobile lipids associated with Triton-resistant membrane domains in haematopoietic K652 cells lacking or expressing caveolin-1. Eur Biophys J 2003, in press.

[47] Delikatny EJ, Couper WA, Brammah S, Sathasivan N, Rideout DC. Nuclear magnetic resonance-visible lipids induced by cationic lipophilic chemotherapeutic agents are accompanied by increased lipid droplet formation and damaged mitochondria. Cancer Res 2002; 62:1394–400.

[48] Martinou JC, Desagher S, Antonsson B. Cytochrome *c* release from mitochondria: all or nothing. Nat Cell Biol 2000;2:E41–3.

[49] Von Ahsen O, Waterhouse NJ, Kuwana T, Newmeyer DD, Green DR. The ''harmless'' release of cytochrome *c*. Cell Death Differ 2000; 7:1192–9.

[50] Wissing D, Mouritzen H, Egeblad M, Poirier GG, Jäättelä M. Involvement of caspase-dependent activation of cytosolic phospholipase A_2 in tumor necrosis factor-induced apoptosis. Proc Natl Acad Sci USA 1997;94:5073–7.

[51] De Valck D, Vercammen D, Fiers W, Beyaert R. Differential activation of phospholipases during necrosis and apoptosis: a comparative study using tumor necrosis factor and anti-Fas antibodies. J Cell Biochem 1997;71:392–9.